Generalized collective modes in a binary He$_{0.65}$-Ne$_{0.35}$ mixture

Taras Bryk,[1,2] Ihor Mryglod,[1] and Gerhard Kahl[2]

[1]*Institute for Condensed Matter Physics, National Academy of Sciences of Ukraine, 1 Svientsitskii Street, UA-290011 Lviv, Ukraine*
[2]*Institut für Theoretische Physik, Technische Universität Wien and CMS, Wiedner Hauptstraße 8-10, A-1040 Wien, Austria*

(Received 24 March 1997)

We have applied the parameter-free collective modes approach to investigate the collective excitation spectra of a He$_{0.65}$-Ne$_{0.35}$ gas mixture at 39.3 K. The static and dynamic correlation functions were calculated directly in molecular dynamics simulations of an ensemble of 864 particles which interact via Aziz potentials. We have compared the spectra calculated within the (basic) hydrodynamic and various extended basis sets of dynamical variables and with results obtained directly from the computer simulation. Within this formalism we were able to obtain ''fast sound'' type modes using an extended hydrodynamic set of seven dynamical variables. A detailed analysis of the contributions of the different spectra of collective modes to the partial dynamical structure factors showed that these ''fast sound'' type excitations appear due to the dynamics of the lighter He particles in the mixture. [S1063-651X(97)00509-6]

PACS number(s): 51.30.+i, 64.75.+g

I. INTRODUCTION

During the last decade essential progress in understanding the dynamical properties of binary systems has been achieved [1–6]. The theoretical and experimental investigations showed that the dynamic structure factors $S(k,\omega)$ of liquid water [1], liquid Li$_4$Pb [2], and of gas mixtures such as He-Ne [3,4] or He-Ar [5,6] display a behavior which can be explained in terms of two pairs of propagating modes, namely so-called ''slow'' and ''fast sound'' modes. The ''slow sound'' excitations (or simply sound excitations) are characterized by a linear dispersion relation in the hydrodynamic region of wave vectors **k** and frequencies ω, while the high-frequency propagating excitations (or ''fast sound'' modes) appear and can be observed for wave numbers k beyond the hydrodynamic region. For the case of liquid water [1] the dispersion relations for the propagating longitudinal (L) and transverse (T) modes have been obtained by fitting the current-current correlation functions $C^{(L,T)}(k,\omega)$ which were calculated in molecular dynamics (MD) simulations: in both cases the excitation spectra contained high-frequency modes. For the He-Ne mixture a different approach has been used in [3]: Here a simple kinetic model, developed within the generalized collective mode approach [7–9] has been proposed; in this model the dynamic structure factor $S(k,\omega)$ is a sum of four Lorentzians, where the parameters have been calculated [3] using a fitting procedure for the *experimental* values of $S(k,\omega)$ of a dense gas mixture of He$_{0.65}$-Ne$_{0.35}$. These results were obtained within the five-mode description of the generalized modes approach where the model contained several fitting parameters.

This contribution is dedicated to an application of the approach of generalized collective modes (Refs. [7–9]) to a binary system. In contrast to [3] our calculations are parameter-free; the only inputs required are the static correlation functions and so-called correlation times determined in MD simulations. This method, which makes investigations of time-correlation functions of fluids possible, represents nowadays a modern and powerful tool: it allows one to obtain the self-consistent description of the dynamical properties in a wide range of wave numbers and frequencies, starting from the hydrodynamic regime up to the Gaussian-like region. Within this framework, time-correlation functions can be written as a weighted sum of partial terms, each of them being associated with a specific generalized collective mode and can be characterized via the corresponding eigenvector and eigenvalue of so-called generalized operators of evolution (see [9,10]). Some of the generalized collective modes correspond in the hydrodynamic limit to the well-known hydrodynamic excitations. The other collective modes with higher eigenvalues are called kinetic modes and have finite damping coefficients in the hydrodynamic region. It is important to note that this approach is based on an *extended* set of dynamic variables which contains, in addition to the conserved variables, their higher-order time derivatives. In general, the required number of the generalized collective modes (or the dynamic variables), which should be taken into account, depends on the considered range in the (k,ω) space; this will be demonstrated in this contribution.

The parameter-free generalized collective mode approach, based on the so-called Markovian approximation for the higher-order memory functions, has been suggested in Ref. [10]: There the five- and seven-variable description of the longitudinal fluctuations for a pure Lennard-Jones liquid has been studied. The extension of the formalism to a nine-variable description has been presented in [11]. The calculation of the time-correlation functions for a Lennard-Jones fluid [12] showed that in a wide range of k and ω a very satisfactory agreement of the theory with MD data can be observed already within the lower-order approximations, i.e., starting from the five-variable description. Similar results have been found for the dynamic correlation functions of liquid Cs near the melting point [13].

One of the attractive features of the generalized mode approach is that it makes it possible to describe propagating kinetic modes which have been observed in some cases in MD or scattering experiments. For instance, it was shown with this method for the transverse current-current correlation function [10–12], that shear waves are in fact propagating kinetic modes. The same conclusion can be drawn about

fast sound modes in the case of binary mixtures [3].

This work is an application of the *parameter-free* generalized collective modes approach to a binary mixture. We concentrate our attention on the study of two main problems: (i) to calculate the collective mode spectrum of a $He_{0.65}$-$Ne_{0.35}$ mixture and to investigate the dependence of the results on the choice of the set of dynamical variables; (ii) to determine the main physical mechanism which forms the fast sound excitations and to study those conditions under which such modes may be observed in the dynamic structure factors.

The paper is organized as follows: Section II outlines the key ideas of the generalized collective modes approach for the case of a binary mixture; in Sec. III we present results of a MD simulation for the static correlation functions and the generalized thermodynamic quantities of a dense gas mixture $He_{0.65}$-$Ne_{0.35}$ at a temperature 39.3 K; the results for the spectra obtained within the generalized collective modes approach and the dynamical structure factors as well as the discussion of the results are given in Sec. IV. The paper is concluded by a summary.

II. THEORETICAL FRAMEWORK

Let us consider a binary mixture in a volume V containing N_1 particles of mass m_1 and N_2 particles of mass m_2. Hence $N_1+N_2=N$ is a total number of particles and

$$c_1=N_1/N, \quad c_2=N_2/N=1-c_1 \tag{1}$$

are the concentrations of the components ''1'' and ''2'' in the mixture.

We now introduce the partial operators of particles of species l ($l=1,2$); for a binary mixture these operators are the partial number densities

$$\hat{n}_l(\mathbf{r},t)=\frac{1}{\sqrt{N}}\sum_{i=1}^{N_l} \delta(\mathbf{r}-\mathbf{r}_i^l(t)), \tag{2}$$

the partial densities of momenta

$$\hat{\mathbf{J}}_l(\mathbf{r},t)=\frac{1}{\sqrt{N}}m_l\sum_{i=1}^{N_l} \mathbf{v}_i^l(t)\delta(\mathbf{r}-\mathbf{r}_i^l(t)), \tag{3}$$

and the partial densities of energies

$$\hat{e}_l(\mathbf{r},t)=\frac{1}{\sqrt{N}}\sum_{i=1}^{N_l} e_i^l(t)\delta(\mathbf{r}-\mathbf{r}_i^l(t)), \tag{4}$$

where

$$e_i^l(t)=\frac{m_l[\mathbf{v}_i^l(t)]^2}{2}+\frac{1}{2}\sum_{l'=1}^{2}\sum_{i'=1}^{N_{l'}}\Phi_{ll'}(|\mathbf{r}_i^l(t)-\mathbf{r}_{i'}^{l'}(t)|). \tag{5}$$

$\mathbf{r}_i^l(t)$ and $\mathbf{v}_i^l(t)$ denote the position and the velocity of particle i of species l at time t, and $\Phi_{ll'}(r)$ is a two-body interaction potential between a particle of species l and a particle of species l' at distance r. The total number density $\hat{n}(\mathbf{r},t)$, the total momentum $\hat{\mathbf{J}}(\mathbf{r},t)$, and the total energy $\hat{e}(\mathbf{r},t)$ are simply defined as the sum of the relevant partial operators:

$$\hat{n}(\mathbf{r},t)=\hat{n}_1(\mathbf{r},t)+\hat{n}_2(\mathbf{r},t),$$

$$\hat{\mathbf{J}}(\mathbf{r},t)=\hat{\mathbf{J}}_1(\mathbf{r},t)+\hat{\mathbf{J}}_2(\mathbf{r},t), \tag{6}$$

$$\hat{e}(\mathbf{r},t)=\hat{e}_1(\mathbf{r},t)+\hat{e}_2(\mathbf{r},t).$$

For an isolated binary system the partial number densities of particles, the density of total momentum, and the density of total energy are conserved quantities. Thus these four microscopic dynamical variables form the so-called hydrodynamic set $\hat{\mathbf{A}}^H(\mathbf{k},t)$,

$$\hat{\mathbf{A}}^H(\mathbf{k},t)=\{\hat{A}_\alpha^H(\mathbf{k},t)\}=\{\hat{n}_1(\mathbf{k},t),\hat{n}_2(\mathbf{k},t),\hat{\mathbf{J}}(\mathbf{k},t),\hat{e}(\mathbf{k},t)\}, \tag{7}$$

where the Fourier transforms $A_\alpha^H(\mathbf{k},t)$ are defined as follows:

$$\hat{n}_l(\mathbf{k},t)=\frac{1}{\sqrt{N}}\sum_{i=1}^{N_l} \exp[i\mathbf{k}\cdot\mathbf{r}_i^l(t)], \tag{8}$$

$$\hat{\mathbf{J}}(\mathbf{k},t)=\hat{\mathbf{J}}_1(\mathbf{k},t)+\hat{\mathbf{J}}_2(\mathbf{k},t), \tag{9}$$

$$\hat{e}(\mathbf{k},t)=\hat{e}_1(\mathbf{k},t)+\hat{e}_2(\mathbf{k},t), \tag{10}$$

and

$$\hat{\mathbf{J}}_l(\mathbf{k},t)=\frac{1}{\sqrt{N}}m_l\sum_{i=1}^{N_l} \mathbf{v}_i^l(t)\exp[i\mathbf{k}\cdot\mathbf{r}_i^l(t)], \tag{11}$$

$$\hat{e}_l(\mathbf{k},t)=\frac{1}{\sqrt{N}}\sum_{i=1}^{N_l} e_i(t)\exp[i\mathbf{k}\cdot\mathbf{r}_i^l(t)]. \tag{12}$$

For the study of the dynamical properties of a binary mixture the hydrodynamic set of dynamical variables (7) should be considered as the smallest and the basic one: With these functions we can describe the behavior of the system correctly in the hydrodynamic region of k and ω, where the processes on a slower time scale are dominant. For intermediate values of k and ω we have to take into account those processes which are realized on a faster time scale: They can now be described within the generalized mode approach by systematically extending the basis set (7) and by considering *extended* sets of dynamic variables which include variables responsible for the processes on this time level. To this purpose, one may—for example—include in addition to the conserved quantities also their time derivatives, as has been demonstrated for a simple fluid [10].

In order to work out the general formalism (independent from the number of dynamic variables to be considered), let us define the square matrix of time-correlation functions $\mathbf{F}^0(k,t)$ using a set of M dynamical variables $\{\hat{A}_1(\mathbf{k},t),\hat{A}_2(\mathbf{k},t),\ldots,\hat{A}_M(\mathbf{k},t)\}$. The elements $F_{ij}^0(k,t)$ of this matrix are given by the correlation functions of two dynamical variables $\hat{A}_i(\mathbf{k},t)$ and $\hat{A}_j(\mathbf{k},t)$ as follows:

$$F_{ij}^0(k,t)=\langle\hat{A}_i(\mathbf{k},0)\hat{A}_j^*(\mathbf{k},t)\rangle, \quad k\neq0. \tag{13}$$

The asterisk denotes complex conjugation and the angular brackets denote the equilibrium ensemble average.

Within the Mori-Zwanzig formalism it is now straightforward to write down the generalized Langevin equation for the matrix $\mathbf{F}^0(k,t)$ [14,15] defined above:

$$\frac{\partial}{\partial t}\mathbf{F}^0(k,t)-i\mathbf{\Omega}(k)\mathbf{F}^0(k,t)+\int_0^\infty \mathbf{M}(k,\tau)\mathbf{F}^0(k,t-\tau)d\tau=0,$$
$$(14)$$

where $i\mathbf{\Omega}(k)$ and $\mathbf{M}(k,\tau)$ are the frequency matrix and the matrix of the memory functions, respectively. This matrix equation can be rewritten in Laplace space as follows:

$$[z\mathbf{I}-i\mathbf{\Omega}(k)+\widetilde{\mathbf{M}}(k,z)]\widetilde{\mathbf{F}}^0(k,z)=\mathbf{F}^0(k,0). \qquad (15)$$

Using the Markovian approximation (denoted by an $\mathcal{M}$) for the memory functions, i.e., $\widetilde{\mathbf{M}}(k,z)\simeq\widetilde{\mathbf{M}}(k,0)$, we obtain the equation

$$[z\mathbf{I}+\mathbf{T}(k)]\widetilde{\mathbf{F}}^\mathcal{M}(k,z)=\mathbf{F}^0(k,t=0), \qquad (16)$$

where the generalized hydrodynamic matrix $\mathbf{T}(k)$ is given by (for details see [10])

$$\mathbf{T}(k)=-i\mathbf{\Omega}(k)+\widetilde{\mathbf{M}}(k,0)\equiv\mathbf{F}^0(k,0)[\widetilde{\mathbf{F}}^0(k,0)]^{-1}, \quad (17)$$

$\mathbf{I}$ is the unit matrix, and $\widetilde{\mathbf{F}}^\mathcal{M}(k,z)$ denotes the matrix of Laplace transforms of time-correlation functions within the Markovian approximation for the memory functions. Using Eq. (16) it is easy to prove the relations

$$\int_0^\infty \mathbf{F}^\mathcal{M}(k,t)dt=\int_0^\infty \mathbf{F}^0(k,t)dt, \qquad (18)$$

$$\mathbf{F}^\mathcal{M}(k,t=0)=\mathbf{F}^0(k,t=0), \qquad (19)$$

which are very important for the sum rules of the time-correlation functions $F_{ij}^\mathcal{M}(k,t)$ (see [12]).

Introducing the eigenvectors $X_{j,\alpha}$ and the eigenvalues z_α of the matrix $\mathbf{T}(k)$ ($j=1,\ldots,M$ and $\alpha=1,\ldots,M$),

$$\sum_{j=1}^M T_{ij}(k)X_{j,\alpha}=z_\alpha(k)X_{i,\alpha}, \quad i=1,\ldots,M \qquad (20)$$

we can write the solution of the matrix equation (16) in the form

$$\widetilde{F}_{ij}^\mathcal{M}(k,z)=\sum_{\alpha=1}^M \frac{G_{ij}^\alpha(k)}{z+z_\alpha(k)}, \qquad (21)$$

where the weight coefficients $G_{ij}^\alpha(k)$ are defined by

$$G_{ij}^\alpha(k)=\sum_{l=1}^M X_{i\alpha}X_{\alpha l}^{-1}F_{lj}^0(k,0). \qquad (22)$$

In time-space the solution (21) has the form

$$F_{ij}^\mathcal{M}(k,t)=\sum_{\alpha=1}^M G_{ij}^\alpha(k)\exp\{-z_\alpha(k)t\}. \qquad (23)$$

Hence we see from Eq. (23) that the time-correlation functions $F_{ij}(k,t)$ calculated in the Markovian approximation via

Eq. (16) can be expressed as a weighted sum over M terms, where each term is characterized by the corresponding eigenvalue $z^\alpha(k)$. The eigenvalues $\{z^\alpha(k)\}$ represent the spectrum of collective modes of the system defined for the set $\{\hat{A}_1(\mathbf{k},t),\hat{A}_2(\mathbf{k},t),\ldots,\hat{A}_M(\mathbf{k},t)\}$.

At this point we have to emphasize that the theoretical approach described above does not contain any adjustable or fitting parameters. Just the Markovian approximation has been assumed, which enables us to obtain the matrix equation (16). As will be seen below, all the elements of the generalized hydrodynamic matrix $\mathbf{T}(k)$ can be expressed via the static correlation functions and the so-called correlation times (both are functions of k only) which, in turn, may be calculated directly in a MD simulation.

In particular, it must be emphasized that the matrix equation (15) is *exact* for *any* set of dynamic variables. The *approximate* equation (16) is derived by applying the Markovian approximation to Eq. (15); hence the results obtained from Eq. (16) will depend on the chosen set of variables.

Thus the study of the dynamic properties of a binary mixture within the generalized mode approach can be divided into the following steps: (i) the choice of the appropriate set of dynamical variables; this depends on the concrete physical situation considered herein [i.e., for instance, the range in (k,ω) space]; (ii) the calculations of all the required matrix elements of $\mathbf{T}(k)$; (iii) the solution of Eq. (16) and calculation of the collective modes spectrum and the time-correlation functions. Beyond that, it can be shown [11,20] that the generalized transport coefficients of the system may also be found within the formalism of the generalized collective modes.

III. GENERALIZED COLLECTIVE MODES APPROACH FOR VARIOUS SETS OF DYNAMICAL VARIABLES

We would like to emphasize that the starting point for our study is the hydrodynamic basis set (7), which consists of conserved variables. It is well known (see, for instance, [14,15]) that one can correctly reproduce the behavior of the hydrodynamic time correlation functions for small values of k and ω in the Markovian approximation for the memory functions using the hydrodynamic variables. In such a case one should expect to find among the hydrodynamic longitudinal collective modes two propagating sound modes and two purely diffusive modes due to the heat and the concentration fluctuations. In a k and ω range *beyond* the hydrodynamic regime we have to take into account memory effects in a more explicit form, i.e., where the dependence of the memory functions on wave number and frequency must be included. This may be achieved in two ways: (i) using some higher-order approximations for the hydrodynamic memory functions, or (ii) applying the Markovian approximation to the higher-order memory functions defined on an extended set of dynamic variables. We shall follow in the next consideration to the second way.

One of the most systematic ways to extend the hydrodynamic set of dynamic variables (7) follows from the projection operator technique [15,10], where a dissipation of the dynamic variables is described mainly via the dynamics of their time derivatives. Hence, we shall consider below the scheme when the extended set of dynamic variables

includes—in addition to the hydrodynamic variables—also the (first) time derivatives of these variables.

A. Hydrodynamic set of dynamic variables

Within the hydrodynamic set of dynamic variables (7) for the longitudinal fluctuations we have to deal with a 4×4 matrix $\mathbf{F}^0(k,t)$. It can be shown that in the static limit $t=0$ the number of the nonzero elements of $\mathbf{F}^0(k)=\mathbf{F}^0(k,0)$ is equal to seven, so that $\mathbf{F}^0(k)$ is a Hermitian matrix and has the form

$$\mathbf{F}^0(k) = \begin{vmatrix} f_{n_1 n_1} & f_{n_1 n_2} & 0 & f_{n_1 e} \\ f_{n_1 n_2} & f_{n_2 n_2} & 0 & f_{n_2 e} \\ 0 & 0 & f_{JJ}^{(L)} & 0 \\ f_{n_1 e} & f_{n_2 e} & 0 & f_{ee} \end{vmatrix}. \quad (24)$$

Since the system is isotropic we have assumed $\mathbf{k}$ to be parallel to the z axis; taking into account the relation

$$\frac{\partial \hat{n}_l(k,t)}{\partial t} = \frac{ik}{m_l} \hat{J}_l^{(L)}(k,t), \quad l=1,2 \quad (25)$$

and using some additional properties of the time-correlation functions [9,10], the matrix $\widetilde{\mathbf{F}}^0(k,z=0)$ can be written in the form

$$\widetilde{\mathbf{F}}^0(k,0) = \begin{vmatrix} \tau_{n_1 n_1} f_{n_1 n_1} & \tau_{n_1 n_2} f_{n_1 n_2} & \dfrac{i}{k}\phi_{nn} & \tau_{n_1 e} f_{n_1 e} \\ \tau_{n_1 n_2} f_{n_1 n_2} & \tau_{n_2 n_2} f_{n_2 n_2} & \dfrac{i}{k}\phi_{nn} & \tau_{n_2 e} f_{n_2 e} \\ \dfrac{i}{k}\phi_{nn} & \dfrac{i}{k}\phi_{nn} & 0 & \dfrac{i}{k}\phi_{ne} \\ \tau_{n_1 e} f_{n_1 e} & \tau_{n_2 e} f_{n_2 e} & \dfrac{i}{k}\phi_{ne} & \tau_{ee} f_{ee} \end{vmatrix}, \quad (26)$$

where

$$\phi_{nn}(k) = m_1 f_{n_1 n_1}(k) + m_2 f_{n_1 n_2}(k), \quad (27)$$

$$\phi_{ne}(k) = m_1 f_{n_1 e}(k) + m_2 f_{n_2 e}(k), \quad (28)$$

and the correlation times $\tau_{ij}(k)$ are defined by the expression

$$\tau_{ij}(k) = \frac{1}{F_{ij}^0(k,0)} \int_0^\infty F_{ij}^0(k,t) dt. \quad (29)$$

B. The extended sets of dynamic variables

The simplest way to extend the hydrodynamic set of dynamic variables (7) is to include in addition to the hydrodynamic variables their first time derivatives. Thus one obtains

the seven-variable set which we shall call the extended hydrodynamic set $\hat{\mathbf{A}}^{EH}(\mathbf{k},t)$ labeled by EH,

$$\hat{\mathbf{A}}^{EH}(\mathbf{k},t) = \{\hat{A}_\alpha^{EH}(\mathbf{k},t)\}$$
$$= \{\hat{n}_1(\mathbf{k},t), \hat{n}_2(\mathbf{k},t), \hat{\mathbf{J}}_1(\mathbf{k},t), \hat{\mathbf{J}}_2(\mathbf{k},t),$$
$$\times \hat{e}(\mathbf{k},t), \dot{\hat{\mathbf{J}}}(\mathbf{k},t), \dot{\hat{e}}(\mathbf{k},t)\}, \quad (30)$$

introducing the new operators

$$\dot{\hat{\mathbf{J}}}(\mathbf{k},t) = \dot{\hat{\mathbf{J}}}_1(\mathbf{k},t) + \dot{\hat{\mathbf{J}}}_2(\mathbf{k},t), \quad (31)$$

$$\dot{\hat{e}}(\mathbf{k},t) = \dot{\hat{e}}_1(\mathbf{k},t) + \dot{\hat{e}}_2(\mathbf{k},t). \quad (32)$$

The microscopic expressions for the operators $\dot{\hat{\mathbf{J}}}_l(\mathbf{k},t)$ and $\dot{\hat{e}}_l(\mathbf{k},t)$ follow directly from Eqs. (3) and (4),

$$\dot{\hat{\mathbf{J}}}_l(\mathbf{k},t) = \frac{1}{\sqrt{N}} \sum_{i=1}^{N_l} m_l \{\mathbf{a}_i^l(t) + i[\mathbf{k}\cdot\mathbf{v}_i^l(t)]\mathbf{v}_i^l(t)\}$$
$$\times \exp[i\mathbf{k}\cdot\mathbf{r}_i^l(t)], \quad l=1,2 \quad (33)$$

$$\dot{\hat{e}}_l(\mathbf{k},t) = \frac{1}{\sqrt{N}} \sum_{i=1}^{N_l} \{\dot{e}_i^l(t) + i[\mathbf{k}\cdot\mathbf{v}_i^l(t)]e_i^l(t)\}$$
$$\times \exp[i\mathbf{k}\cdot\mathbf{r}_i^l(t)], \quad l=1,2 \quad (34)$$

where $\mathbf{a}_i^l(t)$ denotes the acceleration of particle i of species l. We note that using Eqs. (33) and (34) one may directly calculate the corresponding correlation functions of the variables (31) and (32) in a MD experiment (as has been done for a Lennard-Jones fluid in [10]).

In this contribution we shall consider in addition also some other extended sets of dynamic variables in order to investigate the dependence of the results for the collective modes spectrum on the choice of dynamic variables. In Refs. [3,4] the following five-variable set has been used:

$$\hat{\mathbf{A}}^{5A}(\mathbf{k},t) = \{\hat{A}_\alpha^{5A}(\mathbf{k},t)\}$$
$$= \{\hat{n}_1(\mathbf{k},t), \hat{n}_2(\mathbf{k},t), \hat{\mathbf{J}}_1(\mathbf{k},t), \hat{\mathbf{J}}_2(\mathbf{k},t), \hat{e}(\mathbf{k},t)\}. \quad (35)$$

In contrast to Eq. (7) this set of variables includes the partial currents $\hat{\mathbf{J}}_1$ and $\hat{\mathbf{J}}_2$ instead of the total current $\hat{\mathbf{J}}$. By analogy, we may consider another five-variable set where the partial densities of energies $\hat{e}_1$ and $\hat{e}_2$ are included instead of the density of total energy $\hat{e}$, namely,

$$\hat{\mathbf{A}}^{5B}(\mathbf{k},t) = \{\hat{A}_\alpha^{5B}(\mathbf{k},t)\}$$
$$= \{\hat{n}_1(\mathbf{k},t), \hat{n}_2(\mathbf{k},t), \hat{\mathbf{J}}(\mathbf{k},t), \hat{e}_1(\mathbf{k},t), \hat{e}_2(\mathbf{k},t)\}. \quad (36)$$

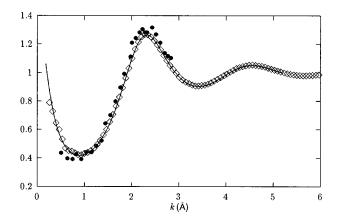As an extention of set (36) one may also introduce the seven-variable set of dynamic variables in the form

FIG. 1. Neutron-weighted total static structure factor $S_{tot}(k)$ for the $He_{0.65}$-$Ne_{0.35}$ mixture investigated in this study. Solid line—integral-equation approach; diamonds—MD data for a 2048 particle ensemble; dots—experimental neutron diffraction data [3].

$$\hat{\mathbf{A}}^{7B}(\mathbf{k},t) = \{\hat{A}_{\alpha}^{7B}(\mathbf{k},t)\}$$

$$= \{\hat{n}_1(\mathbf{k},t), \hat{n}_2(\mathbf{k},t), \hat{\mathbf{J}}(\mathbf{k},t), \hat{e}_1(\mathbf{k},t),$$

$$\times \hat{e}_2(\mathbf{k},t), \dot{\hat{\mathbf{J}}}(\mathbf{k},t), \dot{\hat{e}}(\mathbf{k},t)\}. \quad (37)$$

We see in Eq. (37) that in addition to $\hat{\mathbf{A}}^{5B}(\mathbf{k},t)$ the set of variables $\hat{\mathbf{A}}^{7B}(\mathbf{k},t)$ includes the first time derivatives of $\hat{\mathbf{J}}$ and $\hat{e}$. In this sense, the extended hydrodynamic set $\hat{\mathbf{A}}^{EH}(\mathbf{k},t)$ may also be considered as an extension of the five-variable set $\hat{\mathbf{A}}^{5A}(\mathbf{k},t)$. It is worth noting that the extended hydrodynamic set (30) may be consistently introduced through the time derivatives of the hydrodynamic variables (7).

One of the main goals of this contribution is to find out what different scenarios [corresponding to different ranges in the (k,ω) plane] can be described by using various sets of dynamical variables discussed above; in particular, we would like to study propagating modes in the collective mode spectra in order to find out under which conditions the fast sound excitations can be observed in the dynamic structure factors.

IV. RESULTS AND DISCUSSION

A. Molecular dynamics simulations

We performed MD simulations for a gas mixture of $He_{0.65}$-$Ne_{0.35}$ at a number density $n = 0.0186$ Å^{-3} and at a temperature $T = 39.3$ K, considering a system of 864 particles interacting through Aziz potentials $\Phi_{ll'}(r)$ [16,17] at constant volume $V = L^3$. The potentials were calculated in tabular form on a grid with a mesh size of 0.04 Å. With this kind of interatomic potentials we found the static and dynamic properties of the He-Ne mixture to be in a good agreement with experimental data [4].

The equations of motion were integrated by means of a fourth-order predictor-corrector Gear algorithm with time increment of $\Delta t = 5 \times 10^{-15}$ s. The initial configuration of particles was a face-centered cubic lattice, and the initial velocities were randomly distributed according to a Maxwellian distribution. The melting of the initial configuration and the following thermalization to the desired temperature were performed in 15 000 time steps. The system was observed in

the equilibrium state over a macroscopic time of 1200 ps (240 000 time steps) except for the smallest k value, where it has been extended over 2400 ps (480 000 time steps). Every sixth configuration was taken into account for the computation of the static equilibrium averages. The time correlation functions were calculated by shifting time origins ($\Delta t_0 = 6\Delta t$) on a grid of 2000 points with a step size of $6\Delta t$. Additional averages for the correlation functions have been performed over all N_k possible vectors $\mathbf{k}$ (with $|\mathbf{k}| = k$), which are compatible with the periodic boundary conditions. We have considered 17 wave numbers in the range from $k = k_{min} = 0.175$ Å^{-1} to $k = 25 k_{min}$. Note that the first maximum of the total static structure factor is located at $k_0 \sim 2.15$ Å^{-1}.

B. Static properties

Two pilot calculations have been performed to check the reliability of the calculation of the static averages obtained directly in the MD simulation for the smaller ensemble (864 particles): we compare these data with results for a larger ensemble (2048 particles) and with data obtained in a very accurate integral-equation approach. This integral-equation approach has a modified-hypernetted-chain-type closure relation and is based on the universality hypothesis of the bridge functional (for details we refer the reader to [18,19]). In Fig. 1 we show the total neutron-weighted structure factor

$$S_{tot}(k) = b_1^{*2} c_1 S_{11}(k) + 2 b_1^* b_2^* \sqrt{c_1 c_2} S_{12}(k) + b_2^{*2} c_2 S_{22}(k), \quad (38)$$

where b_1^* and b_2^* are the normalized neutron amplitudes

$$b_l^* = \frac{b_l}{\sqrt{c_1 b_1^2 + c_2 b_2^2}}, \quad l = 1,2 \quad (39)$$

and the $S_{ll'}(k) = f_{n_l, n_{l'}}(k) / \sqrt{c_l c_{l'}}$ are the partial static structure factors, which have been calculated as Fourier trans-
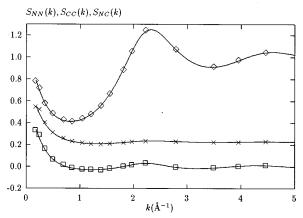

FIG. 2. Bhatia-Thornton static structure factors $S_{NN}(k)$, $S_{NC}(k)$, and $S_{CC}(k)$ for the $He_{0.65}$-$Ne_{0.35}$ mixture investigated in this study: the results obtained by the integral-equation approach are shown by solid curves; MD data for an 864 particle ensemble are represented by symbols [diamonds—$S_{NN}(k)$; crosses—$S_{CC}(k)$; boxes—$S_{NC}(k)$].

forms of the MD partial pair correlation functions and/or from the data obtained via the integral-equation method. The comparison with the experimental results [3] of neutron diffraction experiments on He$_{0.65}$-Ne$_{0.35}$ is shown in Fig. 1 and one may see that the position and the magnitude of the first peak are in good agreement with the experimental data. Hence we may conclude that the results of two pilot calculations (Fig. 1 and the upper curve in Fig. 2) performed for the 864 and 2048 particle ensembles are in good agreement and correlate well with the experimental data and the results of the integral-equation method. It is worth noting that the specific behavior of the static structure factor observed in the range of small k values is typical for a system which is close to the demixing transition.

All the static correlation functions required for the calculation of the generalized hydrodynamic matrix $\mathbf{T}(k)$ have been obtained directly in MD simulations. The correlation times τ_{ij} have been calculated directly via Eq. (29). In this section we shall present results for the static structure factors and the generalized thermodynamic quantities (defined below) which are expressed via static correlation functions and tend to the well-known thermodynamic expressions when $k \to 0$.

The Bhatia-Thornton structure factors can be expressed via the static correlation functions calculated directly in MD simulations [20–22],

$$S_{NN}(k) = f_{nn}(k), \tag{40}$$

$$S_{NC}(k) = f_{n_1 n}(k) - c_1 f_{nn}(k), \tag{41}$$

$$S_{CC}(k) = f_{n_1 n_1}(k) - 2c_1 f_{n_1 n}(k) + c_1^2 f_{nn}(k). \tag{42}$$

Using these definitions the $S_{NN}(k)$, $S_{NC}(k)$, and $S_{CC}(k)$ tend for large k to 1, 0, and $c_1 c_2$, respectively. Results for $S_{NN}(k)$, $S_{NC}(k)$, and $S_{CC}(k)$ are shown in Fig. 2 by diamonds, boxes, and crosses, respectively.

The generalized thermodynamic quantities as functions of k investigated in this study are the generalized isothermal compressibility $\kappa_T(k)$, the generalized second derivatives of the Gibbs potential (see [21]) or so-called Z factors [$Z_P(k)$ and $Z_V(k)$], the generalized "$N-C$" dilatation $\delta(k)$ (see [21]), the generalized thermal expansion coefficient $\alpha(k)$, the generalized specific heat at constant volume $C_V(k)$, and the generalized ratio of specific heats $\gamma(k)$ at constant volume and constant pressure; they are plotted in Fig. 3. The closed expressions for these quantities have been derived [20] on the basis of the thermodynamic theory of fluctuations and can be written as follows (k_B is the Boltzmann constant):
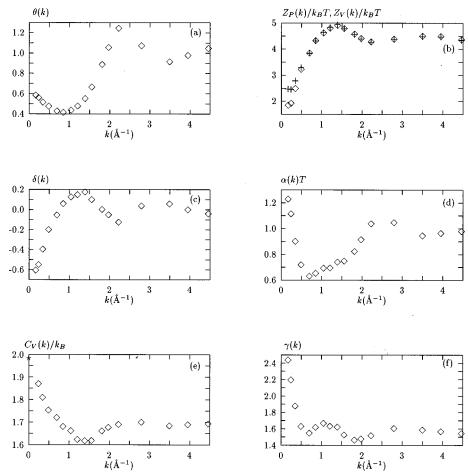

FIG. 3. Generalized thermodynamic quantities for the He$_{0.65}$-Ne$_{0.35}$ mixture at $T = 39.3$ K: (a) generalized compressibility $\theta(k)$; (b) generalized factors $Z_V(k)$ (+) and $Z_P(k)$ (□); (c) generalized $N-C$ dilatation $\delta(k)$; (d) generalized linear expansion coefficient $\alpha(k)$; (e) generalized specific heat at constant volume $C_V(k)$ (the asterisk for $k=0$ points at MD value for C_V calculated via temperature fluctuation in the MD simulation); (f) generalized ratio of specific heats $\gamma(k)$.

$$\theta(k) = \frac{N}{V} k_B T \kappa_T(k) = \frac{f_{nn}(k) \widetilde{f}_{n_1 n_1}(k)}{S_{CC}(k)} \quad \text{and}$$

$$\lim_{k \to 0} \theta(k) = \frac{N}{V} k_B T \kappa_T \qquad (43)$$

for the generalized compressibility $\kappa_T(k)$ [see Fig. 3(a)], where

$$\kappa_T = -\frac{1}{V} \left(\frac{\partial V}{\partial P} \right)_{T,N,N_1} \qquad (44)$$

and

$$\widetilde{f}_{n_1 n_1}(k) = f_{n_1 n_1}(k) - \frac{f_{n_1 n}^2(k)}{f_{nn}(k)}, \qquad (45)$$

$$Z_P(k) = \frac{k_B T}{S_{CC}(k)}, \quad Z_V(k) = \frac{k_B T}{\widetilde{f}_{n_1 n_1}(k)}, \quad \text{and}$$

$$\lim_{k \to 0} Z_P(k) = \frac{1}{N} \left(\frac{\partial^2 G}{\partial c_1^2} \right)_{P,T,N} \qquad (46)$$

for the generalized $Z_P(k)$ and $Z_V(k)$ factors [see Fig. 3(b)], where G is the Gibbs potential;

$$\delta(k) = -\frac{S_{NC}(k)}{S_{CC}(k)} \quad \text{and} \quad \lim_{k \to 0} \delta(k) = \frac{V_1 - V_2}{V} \qquad (47)$$

for the generalized $N - C$ dilatation [see Fig. 3(c)];

$$\alpha(k) T = \frac{N}{V} \frac{\kappa_T(k)}{i k k_B T} \widetilde{f}_{je}^{(L)}(k) \quad \text{and}$$

$$\lim_{k \to 0} \alpha(k) = \frac{1}{V} \left(\frac{\partial V}{\partial T} \right)_{P,N_1,N_2} \qquad (48)$$

for the generalized thermal expansion coefficient $\alpha(k)$ [see Fig. 3(d)], where

$$\widetilde{f}_{je}^{(L)}(k) = \widetilde{f}_{je}^{(L)}(k) - i k k_B T \left(\frac{f_{ne}(k)}{f_{nn}(k)} - \frac{\widetilde{f}_{n_1 e}(k)}{\widetilde{f}_{n_1 n_1}(k)} \frac{S_{NC}(k)}{f_{nn}(k)} \right) \qquad (49)$$

and

$$\widetilde{f}_{n_1 e}(k) = f_{n_1 e}(k) - f_{ne}(k) \frac{f_{n_1 n}(k)}{f_{nn}(k)}, \qquad (50)$$

$$C_V(k) = \frac{1}{k_B T^2} \left(f_{ee}(k) - \frac{f_{ne}^2(k)}{f_{nn}(k)} - \frac{\widetilde{f}_{n_1 e}^2(k)}{\widetilde{f}_{n_1 n_1}(k)} \right) \quad \text{and}$$

$$\lim_{k \to 0} C_V(k) = C_{V,N,N_1} \qquad (51)$$

for the generalized specific heat at constant volume [see Fig. 3(e)];

$$\gamma(k) = 1 + \frac{[\alpha(k)T]^2}{\theta(k)} \frac{k_B}{C_V(k)} \qquad (52)$$

for the generalized ratio of specific heats [see Fig. 3(f)]. For the k dependence of these quantities one may observe the following.

(i) The reduced generalized compressibility $\theta(k)$ [Fig. 3(a)] differs from $S_{NN}(k)$ (plotted in Fig. 2) in the region $k < 0.7$ Å^{-1}. Note that

$$\lim_{k \to 0} S_{NN}(k) = \frac{N}{V} k_B T \kappa_{T,\mu} = -\frac{1}{V} \left(\frac{\partial V}{\partial P} \right)_{T,N,\mu},$$

where $\kappa_{T,\mu}$ is a compressibility given in (P,T,N,μ) ensemble.

(ii) The curves of $Z_P(k)$ and $Z_V(k)$ [Fig. 3(b)] coincide for $k > 1.5$ Å^{-1} but differ in the region of small k.

(iii) The generalized $N - C$ dilatation [Fig. 3(c)] becomes negative for $k \to 0$ because the particles of the first species (Ne) are heavier.

(iv) The generalized thermal expansion coefficient [Fig. 3(d)] decreases rapidly for small values of k ($k < 0.5$ Å^{-1}) as the wave number increases, while for larger k values it has a maximum at the position of the main peak of $S_{NN}(k)$. Such a behavior can also be observed in pure liquids [10,13].

(v) The extrapolated value of $C_V(k)$ for $k \to 0$ [Fig. 3(e)] is in good agreement with the value obtained from MD data via the fluctuation formula (marked by an asterisk).

(vi) In the hydrodynamic region the generalized ratio of specific heats $\gamma(k)$ is rapidly decreasing as a function of k.

We note the following.

(1) The difference between the functions $\theta(k)$ and $S_{NN}(k)$ as well as the functions $Z_P(k)$ and $Z_V(k)$ is due to the difference between the fluctuation formulas of the same quantity defined in various ensembles. This difference is proportional to the ratio $\widetilde{f}_{n_1 n_1}(k)/S_{CC}(k)$ in both cases and tends to zero as k becomes larger.

(2) The coupling of thermal and viscous processes is mainly described by the generalized thermal expansion coefficient $\alpha(k)$. Comparing the behavior of $\alpha(k)$ for a mixture He$_{0.65}$-Ne$_{0.35}$ and for a simple fluid (see, e.g., [10,13]) in the range of k smaller than k_0 (see above), one may conclude that the energy fluctuations play an important role for the system considered here.

(3) Using the extrapolated values of $\gamma(k)$ and $\kappa_T(k)$ for $k \to 0$, we can calculate the adiabatic velocity of sound [21] defined by the expression

$$c_s = \left(\frac{\gamma}{\rho K_T} \right)^{1/2}, \qquad (53)$$

where ρ is the mass density. In such a manner (and depending on the extrapolation procedure) we have found values for c_s which are within the range of 300–350 m/s. As will be seen below these values correlate well with the results obtained from the study of the spectra of the generalized collective modes in the hydrodynamic limit. Using Eq. (53) for the values of $\gamma(k)$ and $\kappa_T(k)$ taken, respectively, at the
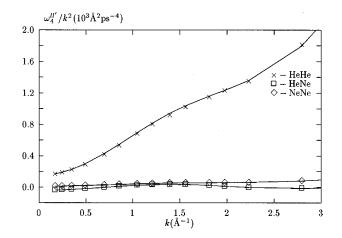
FIG. 4. Fourth frequency moments of the partial dynamical structure factors divided by k^2 as functions of k for the $He_{0.65}$-$Ne_{0.35}$ mixture investigated in this study: solid lines—calculated using the partial radial distribution functions; symbols—calculated directly in the MD simulation as static averages $f_{j_l j_{l'}}^{(L)}$ (crosses—He-He; boxes—He-Ne; diamonds—Ne-Ne).

smallest k (i.e., $k_{min} = 0.1748$ Å^{-1}) we obtain $c_s = 376.9$ m/s which is close to the value 362 m/s obtained from a phenomenological equation of state (see references in [3]). However, it should be noted that the value k_{min} lies in fact *outside* the hydrodynamic region of wave numbers as will be seen from the spectra of the generalized collective modes: At this k point already new propagating *kinetic* modes appear which can be identified as fast sound modes.

C. Dynamical properties

In this section we present the numerical results for the dynamic structure factors and the spectra of the longitudinal collective modes calculated within the generalized mode approach. It should be noted once again that all the required quantities which form the generalized hydrodynamic matrix have been obtained directly in a MD experiment, so that neither adjustable nor fitting parameters were required or used. To illustrate the internal consistency of our approach we plotted in Fig. 4 the k dependence of the fourth frequency moments $\omega_4^{ll'}(k)$ of the partial dynamic structure factors divided by k^2: We display the values calculated directly in the MD simulation as the static averages $f_{j_l j_{l'}}^{(L)}$, ($l,l' =$ He, Ne) and the values $\omega_4^{ll'}/k^2$ calculated via the partial radial distribution functions and the derivatives of interatomic potentials on the basis of well-known expressions (see, e.g., [14]). One may see in Fig. 4 that the results are in very good agreement. In addition we point out that, for example, the time-correlation function $F_{nn}(k,t)$, calculated on the basis of the extended hydrodynamic set (30), gives the exact values for the frequency moments up to fourth order, due to the fact that the first time derivatives of the hydrodynamic variables are taken into account explicitly in this case (see also [12]). Hence we expect that the short-time behavior of the time-correlation functions will be described more precisely within the extended hydrodynamic set.

In Figs. 5 we compare the partial density-density time-correlation functions calculated in the MD simulation (open
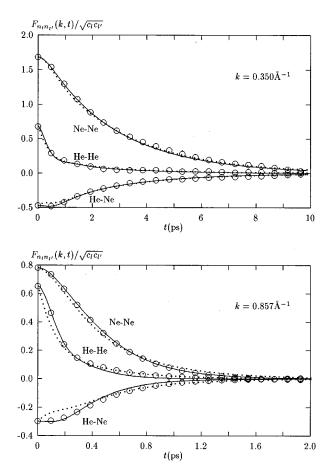

FIG. 5. Partial density-density correlation functions for two fixed values of k for the $He_{0.65}$-$Ne_{0.35}$ mixture investigated in this study: open circles—MD data; dotted lines—the results obtained for the hydrodynamic set of variables (7); solid lines—the results for the extended hydrodynamic set of variables (30).

circles) with those obtained within the generalized mode approach for the hydrodynamic [$\hat{\mathbf{A}}^H(k)$—dotted curve] and extended hydrodynamic [$\hat{\mathbf{A}}^{EH}(k)$—solid curve] sets of dynamic variables. The results are given at two wave numbers k, namely, $k = 0.350$ Å^{-1} and $k = 0.857$ Å^{-1} (both of them are much smaller than k_0). In Figs. 5 it is clearly seen that the results obtained within the extended hydrodynamic set provide a much better agreement with MD data compared to the results for the hydrodynamic set (7); the difference becomes—as expected—more pronounced for larger values of k.

The spectra of the generalized collective modes obtained for the hydrodynamic (7) and the extended hydrodynamic (30) sets of dynamic variables are shown in Figs. 6. The eigenvalues z_α are given in reduced units, using the time scale τ_σ,

$$\tau_\sigma = \frac{1}{k_{min}} \sqrt{\frac{c_1 m_1 + c_2 m_2}{k_B T}}.$$

As expected, we found for the hydrodynamic set $\hat{\mathbf{A}}^H(k)$ [Figs. 6(a) and 6(b)] four generalized modes, which can be considered as the extension of usual hydrodynamic modes known in the literature (see, e.g., [21]). In the hydrodynamic
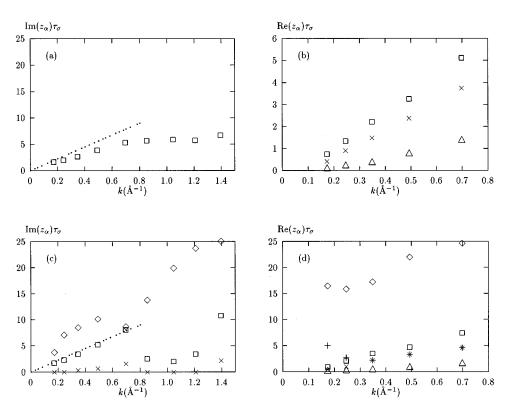
FIG. 6. Spectra of eigenvalues obtained for the hydrodynamic set of variables (7) (a), (b) and the extended hydrodynamic set of variables (30) (c), (d) for the $He_{0.65}$-$Ne_{0.35}$ mixture investigated in this study. The linear dispersion of sound with $c_s = 362$ m/s (see [3]) is plotted by a dotted line. The imaginary (a), (c) and real (b), (d) parts of the eigenvalues are shown by symbols [sound modes by boxes; concentration modes (b), (d) by triangles; fast sound modes (c), (d) by diamonds; the pair of propagating modes (c), (d), which transform at small values of k into two purely diffusive modes by $\times$ and $+$]. The time scale unit τ_σ (see text) is given by 3.109 ps.

limit $k \to 0$ these modes are (i) two complex conjugated propagating modes which correspond to sound excitations with the eigenvalues

$$z_s^\pm = \Gamma k^2 \pm i c_s k, \tag{54}$$

where c_s and Γ are the velocity and damping coefficient of the sound excitations, respectively; (ii) two purely diffusive modes describing the concentration (c) and heat (h) fluctuations

$$z_c = D_c k^2, \tag{55}$$

$$z_h = D_h k^2, \tag{56}$$

where D_c and D_h are the concentration damping coefficient and the heat diffusivity, respectively. Our estimates, obtained for k_{min} within the hydrodynamic set (7), give $c_s = 286.7$ m/s, $\Gamma = 7.52 \times 10^{-8}$ m^2/s, $D_c = 0.80 \times 10^{-8}$ m^2/s, $D_h = 4.37 \times 10^{-8}$ m^2/s. Furthermore, it should be noted that one can also extract the transport coefficients using the known expressions [21], which relate the hydrodynamic eigenvalues to these transport coefficients (the viscosity, the concentration diffusion coefficient D, and the thermal conductivity κ).

The spectra of the generalized collective modes calculated within the extended hydrodynamic set $\hat{A}^{EH}(k)$ are shown in Figs. 6(c) and 6(d). In this case we obtained seven eigenvalues z_α which describe the time dependence of the system [cf. Eq. (23)]. In the hydrodynamic limit, we find (as it should

be) in addition to the previous results [Eqs. (54)–(56)] two relaxing kinetic modes $z_{k1}(k)$ and $z_{k2}(k)$ [denoted by $+$ and $\diamond$ in Fig. 6(d)] with finite damping coefficients,

$$\lim_{k \to 0} [\mathrm{Re} z_{k1}(k)] = z_{k1}^0 > 0, \quad \lim_{k \to 0} [\mathrm{Re} z_{k2}(k)] = z_{k2}^0 > 0.$$

The kinetic modes describe processes of a subsequent time scale, i.e., faster processes in comparison with the hydrodynamic ones.

In Fig. 6(d) we can see that for large values of k there exist one purely real relaxing mode, which may be considered as the extended concentration mode (triangles), and three pairs of complex conjugated propagating modes, one of which corresponds to the generalized sound excitations (boxes). The other two pairs of propagating modes reduce to the modes with purely real eigenvalues as k decreases.

(i) For $k \leq 0.3$ Å^{-1} the imaginary part of the eigenvalues for the propagating kinetic modes [denoted by $\times$ in Fig. 6(c)] becomes zero, and they degenerate for smaller values of k into two relaxing modes [denoted by $\times$ and $+$ in Fig. 6(d)], one of which is an extension of the heat mode. Note that the dispersion of these modes for $k > 0.3$ Å^{-1} is always below $\omega_s(k) = c_s k$ [dotted line in Fig. 6(c)].

(ii) The third pair of propagating modes (plotted by diamonds) with the largest real part of the eigenvalues behave in the range of small and intermediate values of k similar to the fast sound modes found in [3,4]. This means that the dispersion of these modes, $\omega_k(k)$, is larger than the dispersion of the sound modes $\omega_s(k)$ for all the values of k con-

sidered in the simulations; however, there is a clear tendency that $\omega_k(k)$ tends to zero as k tends to k_H from above, so that for $k < k_H$ these modes reduce to two relaxing kinetic modes with purely real eigenvalues [where the value k_H can be defined by the equation $\omega_k(k_H) = 0$]. From Fig. 6(c) one may estimate the value of k_H to be $k_H \simeq 0.1$ Å^{-1}. Due to the finite size of our ensemble (introducing thus k_{min}) we are not able to give a more accurate result for k_H. Such properties are in agreement with the conclusion given in [3].

We also list our estimates for the quantities which describe the behavior of the generalized hydrodynamic mode as k tends to 0, obtained within the extended hydrodynamic set (30): $c_s = 296.5$ m/s, $\Gamma = 9.11 \times 10^{-8}$ m^2/s, $D_c = 0.81 \times 10^{-8}$ m^2/s, $D_h = 4.59 \times 10^{-8}$ m^2/s. These values correlate well with the estimates found for the hydrodynamic set of dynamic variables.

Summarizing, one may conclude that the fast sound excitations which have been observed experimentally [2,3] in binary mixtures can be described within the generalized mode approach on the basis of the extended hydrodynamic set $\hat{\mathbf{A}}^{EH}(k)$. We add that a similar behavior of the propagating kinetic modes has also been found for a Lennard-Jones fluid [11]. However, in the case of simple liquids the dispersion of the propagating kinetic modes was below $\omega_s(k)$, so that these modes were not directly visible in the dynamic structure factor.

Therefore, in an effort to find more precisely the reasons under which conditions the fast sound solutions appear we consider in the following also the other sets of dynamical variables discussed above [see Eqs. (35)–(37)]. Such investigations are also motivated by the fact that such a kind of solution has been found previously [3,4] within the variable set (35), using the seven-parameter fitting procedure for the elements of the generalized hydrodynamic matrix.

Before analyzing the results we note that for any set of dynamical variables which includes the conserved hydrodynamic variables, the spectra of the collective modes must describe correctly the hydrodynamic behavior. This means that four of the eigenvalues should be hydrodynamic eigenvalues [which, in the limit $k \to 0$, describe two complex conjugated propagating modes (sound excitations)] and two eigenvalues should be purely diffusive ones [see Eqs. (54)–(56)]. The other collective modes have to be kinetic ones with finite damping coefficients as k tends to 0; they contribute only to the central peaks (located at $\omega = 0$) of dynamical structure factors when k is small.

The results for spectra of the generalized collective modes obtained within various sets of dynamic variables $\hat{\mathbf{A}}^{5A}(k)$, $\hat{\mathbf{A}}^{5B}(k)$, and $\hat{\mathbf{A}}^{7B}(k)$ are shown in Fig. 7. (i) In Fig. 7(a) the imaginary parts of the eigenvalues, calculated for the set (35), are plotted. In this case and for $k > 0.4$ Å^{-1} we found two pairs of propagating modes and one mode with a purely real eigenvalue: The first pair describes sound excitations; the second pair of propagating modes decomposes into two relaxing modes when k is smaller than 0.4 Å^{-1}: one of them is the heat mode and the other one is a kinetic mode. Hence the general behavior of solving the eigenvalue problem for the set $\hat{\mathbf{A}}^{5A}(k)$ is very similar to that found in [3]. However, it is seen in Fig. 7(a) that in contrast to [3] these modes cannot be considered as fast sound excitations. More likely
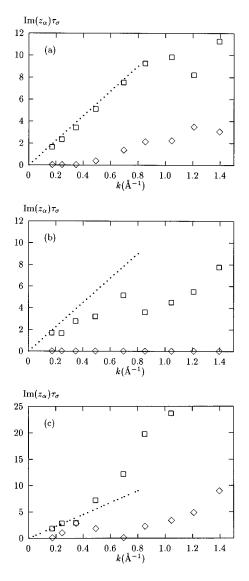

FIG. 7. Imaginary parts of the eigenvalues obtained for the various sets $\hat{\mathbf{A}}^{5A}$, $\hat{\mathbf{A}}^{5B}$, and $\hat{\mathbf{A}}^{7B}$ of dynamic variables, namely, (a) for Eq. (35), (b) for Eq. (36), and (c) for Eq. (37). The dispersions of sound and propagating kinetic modes are shown by boxes and diamonds, respectively. The time scale unit τ_σ is given in the caption of Fig. 6.

they are related to the kinetic propagating modes found for the extended hydrodynamic set [compare the low-lying curves in Fig. 7(a) and Fig. 6(c)]. (ii) The imaginary parts of the eigenvalues, calculated for the set $\hat{\mathbf{A}}^{5B}(k)$ where the partial densities of the energies are taken into account, are shown in Fig. 7(b). In the entire range of k considered, we do not find any other propagating modes at all [except for sound modes (plotted by boxes)]. (iii) For the set $\hat{\mathbf{A}}^{7B}(k)$ such modes appear again for $k > 0.2$ Å^{-1} [see Fig. 7(c)]. We emphasize that set (37) can be considered as an extension of set (36), so that we now might expect to obtain more accurate results for the low-lying collective modes. However, propagating kinetic modes, which could be identified as fast sound excitations, have not been found. Thus we conclude that *only the extended hydrodynamic set $\hat{\mathbf{A}}^{EH}(k)$ of dynamical variables provides a way to describe fast sound modes.*

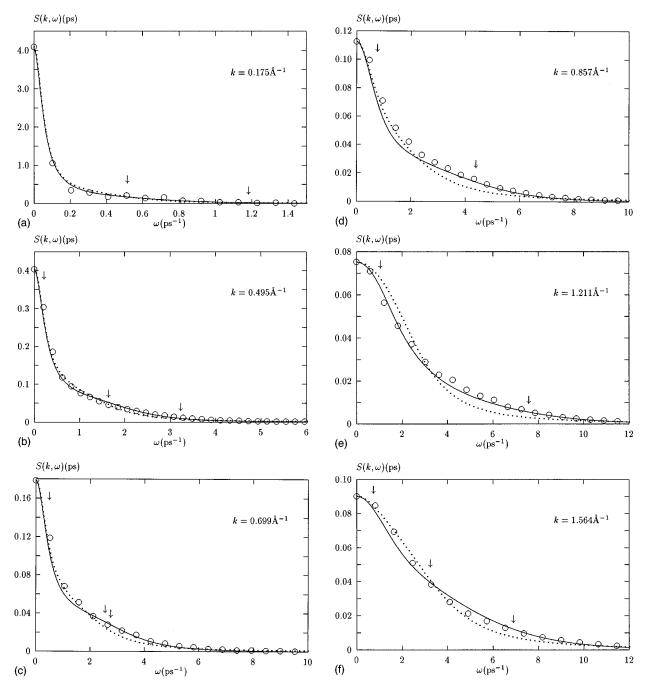Let us consider now the results for the partial dynamical

FIG. 8. Total neutron-weighted dynamic structure factors (58) for six different values of k obtained within the hydrodynamic set (7) (dotted curves), the extended hydrodynamic set (30) (solid curves), and by numerical Fourier transformation of MD data (open circles). Arrows display values of the imaginary parts of eigenvalues for propagating modes obtained within the extended hydrodynamic set (30).

structure factors. As follows from Eq. (23) we get

$$S_{ll'}(k,\omega) = \frac{1}{\pi\sqrt{c_l c_{l'}}} \mathrm{Re}\left[\sum_{\alpha=1}^{M} \frac{G_{n_l n_{l'}}^{\alpha}(k)}{i\omega + z_{\alpha}(k)} \right]. \qquad (57)$$

Using Eqs. (38) and (57) one can calculate the total neutron-weighted dynamic structure factor $S_{\mathrm{tot}}(k,\omega)$ for our system,

$$S_{\mathrm{tot}}(k,\omega) = \frac{1}{\pi} \mathrm{Re}\left[\sum_{\alpha=1}^{M} \frac{\mathcal{G}^{\alpha}}{i\omega + z_{\alpha}(k)} \right], \qquad (58)$$

where the coefficients $\mathcal{G}^{\alpha}$ are the corresponding linear combinations of the $G_{n_l n_{l'}}^{\alpha}$.

In Fig. 8 the total dynamic structure factor $S_{\mathrm{tot}}(k,\omega)$ calculated with the hydrodynamic set $\hat{\mathbf{A}}^{H}(k)$ and the extended hydrodynamic $\hat{\mathbf{A}}^{EH}(k)$ sets are plotted for six different values of k (dotted and solid curves, respectively); MD data are shown by open circles. The positions of the propagating modes found for the extended hydrodynamic set are shown by arrows. We see that the results obtained within the seven-variable approximation of the generalized collective mode approach agree well with MD data for all the considered values of k. The hydrodynamic set gives results which agree
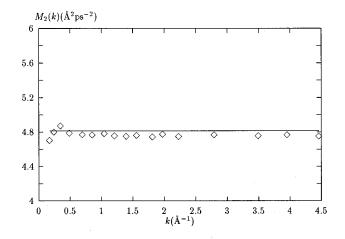
FIG. 9. Second frequency moment $M_2(k)$ of the total dynamic factor (diamonds) calculated in comparison with the theoretical value (solid line).

FIG. 11. Partial dynamic structure factors obtained for the extended hydrodynamic set (30) (solid curves). The dotted curves show the partial dynamic structure factors if the contribution from the fast sound like modes is neglected.

with computer simulation data only for small k's, which shows clearly that, as k is increased, the nonhydrodynamic effects become more important. One can see in Fig. 8 that for $k = 0.699$ Å^{-1} and $k = 0.857$ Å^{-1} the contributions from the propagating kinetic modes, which may be identified as fast sound modes, are visible (the positions of fast sound excitations are shown by arrows on the right-hand side). For smaller wave numbers ($k < 0.7$ Å^{-1}) these modes can no longer be observed because the contributions from the kinetic modes in Eqs. (57) and (58) are proportional to k^2 and the damping coefficient is too large. On the other hand, for $k > 0.9$ Å^{-1} the fast sound modes are not visible either, due to the increasing damping coefficient. Still, one may conclude from the results in Fig. 8 that for large values of k the fast sound excitations should be taken into account for a correct description of the dynamic structure factor: they improve the accuracy in the range of intermediate values of k and ω.

In Figs. 9 and 10 the results for second frequency moment $M_2(k)$ of the total dynamic structure factor calculated within the extended hydrodynamic set,

$$M_2(k) = \frac{\omega_2^{tot}(k)}{k^2} = \frac{1}{k^2} \int_{-\infty}^{\infty} \omega^2 S_{tot}(k,\omega) d\omega,$$

and the half-width at half height $\omega_H(k)$ are plotted as functions of k, respectively. Within the accuracy of 2% the second frequency moment (diamonds in Fig. 9) is in a good agreement with the theoretical value (see [3]) shown by a solid line. In Fig. 10 the half-width at half height of $S_{tot}(k,\omega)$ (diamonds) in the region of small k values is a function proportional to k^2, as it should be. Two dotted lines in Fig. 10 are the functions $D_h k^2$ (upper dotted line) and $D_c k^2$ (lower dotted line), where D_h and D_c are the values of thermodiffusion (56) and concentration diffusion (55) coefficients, respectively. In binary systems the width of the central peak of $S_{tot}(k,\omega)$ in the hydrodynamic region depends on interplay between thermodiffusion and concentration diffusion processes. Therefore for small values of k the function $\omega_H(k)$ is in between the dotted curves.

In order to investigate the influence of the high-frequency propagating kinetic modes (fast sound) on the partial dynamical structure factors we display in Fig. 11 $S_{ll'}(k,\omega)$ ($l,l' =$ He, Ne), using the extended hydrodynamic set $\hat{\mathbf{A}}^{EH}(k)$. There the partial dynamic structure factors are plotted for $k = 0.857$ Å^{-1}, i.e., for k values when the fast sound modes could be clearly identified in the total dynamic structure factor (see above and Fig. 8). We present results for $S_{ll'}(k,\omega)$: the full line represents the sum (57) containing *all* terms, while the broken line shows data when the contribution from the fast sound modes is neglected. It is obvious that the fast sound contribution affects mainly the dynamics of lighter He particles and has no visible effect on the dynamics of the heavier Ne particles. This is consistent with the conclusion made previously in Refs. [2,3].
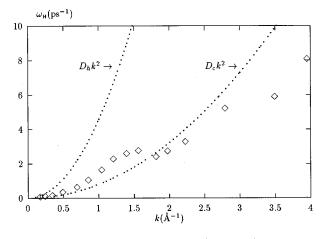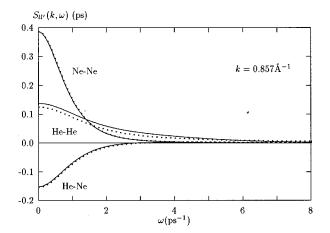

FIG. 10. Half-width at half height ω_H (diamonds) calculated for the total dynamic structure factor. The pure contributions from the thermodiffusion and concentration diffusion terms [see Eq. (58)] are plotted by upper and lower dotted lines, respectively.

V. CONCLUSION

In the present paper, the generalized collective mode approach, extended to binary mixtures in the parameter-free form, has been applied to study the dynamical properties of a

He $_{0.65}$-Ne $_{0.35}$ mixture. In particular, the spectra of the generalized collective modes have been studied for various sets of dynamical variables. Our main concern was to investigate the excitations of fast soundlike modes, described previously in [3,4]: We recall that such excitations have been obtained in [3,4] using a seven-parameter fitting procedure for the set of variables (35).

One of the most important aspects of our results is that from all the sets of dynamical variables considered in this study the appearance of fast sound modes can only be described within the *extended hydrodynamic* set (30). For all the other sets we have not found modes which could be identified as fast sound modes. We recall that in contrast to the *exact* formalism [see Eq. (15)], where all sets of dynamical variables are equivalent, the Markovian approximation, which is the key point of the generalized mode approach, brings along that these sets are no longer equivalent. However, as has been shown for pure liquids in Refs. [12], by extending a set of dynamical variables by including their time derivatives the following is observed: the short-time kinetic properties can be described more precisely and a tendency for the convergence of the results for the collective modes spectra as well as a better agreement of the time-correlation functions with MD data in the generalized mode approach is observed. In contrast to the other sets considered here, the extended hydrodynamic set (30) is the most natural one because it contains all the first time derivatives of the hydrodynamic variables and therefore short-time kinetic processes of the same scale are considered.

Furthermore, it has been shown that the parameter-free generalized mode approach for the extended hydrodynamic set $\hat{\mathbf{A}}^{EH}$ gives results for the time-correlation functions (such as the dynamic structure factors) which are in good agreement with MD data. In our study it has been found that the condition under which the fast sound excitations may be observed depends on the ratio of the damping coefficients as a function of k. From the physical point of view the fast sound modes are found to be closely connected with the dynamics of the lighter component in a mixture.

Based on the results given here, further time-correlation functions and generalized transport coefficients, such as the generalized shear and bulk viscosities, the generalized thermal conductivity, and the generalized diffusion coefficient, can be computed. It would also be interesting to investigate the spectra of generalized collective modes in higher approximations, taking into account second- and higher-order time derivatives of the hydrodynamic variables, since it has been shown for simple fluids [11,12] that in this way the low-lying eigenvalues can be reproduced with higher accuracy. We plan to present results of such a study (extension to the binary case) elsewhere.

[1] U. Balucani, J. P. Brodholt, and R. Vallauri, J. Phys. Condens. Matter **8**, 9269 (1996).

[2] J. Bosse, G. Jacucci, M. Ronchetti, and W. Schirmacher, Phys. Rev. Lett. **57**, 3277 (1986).

[3] P. Westerhuijs, W. Montfrooij, L. A. de Graaf, and I. M. de Schepper, Phys. Rev. A **45**, 3749 (1992).

[4] P. Westerhuijs, Ph.D. thesis, Technische Universiteit Delft, 1992.

[5] H. E. Smorenburg, R. M. Crevecoeur, and I. M. de Schepper, Phys. Lett. A **211**, 118 (1996).

[6] H. Smorenburg, Ph.D. thesis, Technische Universiteit Delft, 1996.

[7] W. E. Alley and B. J. Alder, Phys. Rev. A **27**, 3158 (1983).

[8] B. Kamgar-Parsi, E. G. D. Cohen, and I. M. de Schepper, Phys. Rev. A **35**, 4781 (1987).

[9] I. M. de Schepper, E. G. D. Cohen, C. Bruin, J. C. van Rijs, W. Montfrooij, and L. A. de Graaf, Phys. Rev. A **38**, 271 (1988).

[10] I. M. Mryglod, I. P. Omelyan, and M. V. Tokarchuk, Mol. Phys. **84**, 235 (1995).

[11] I. P. Omelyan and I. M. Mryglod, Condens. Matt. Phys. (Ukraine) **N4**, 128 (1994); I. M. Mryglod and I. P. Omelyan, Phys. Lett. A **205**, 401 (1995).

[12] I. M. Mryglod and I. P. Omelyan, Mol. Phys. **90**, 91 (1997); and to be published.

[13] T. Bryk and Y. Chushak, J. Phys. Condens. Matter **9**, 3329 (1997).

[14] J.-P. Boon and S. Yip, *Molecular Hydrodynamics* (McGraw-Hill, New York, 1980).

[15] J.-P.Hansen and I. R. McDonald, *Theory of Simple Liquids* (Academic, London, 1986).

[16] R. A. Aziz, F. R. W. McCourt, and C. C. K. Wang, Mol. Phys. **61**, 1487 (1987).

[17] R. A. Aziz and N. J. Slaman, Chem. Phys. **130**, 187 (1989).

[18] G. Kahl, B. Bildstein, and Y. Rosenfeld, Phys. Rev. E **54**, 5391 (1996).

[19] Y. Rosenfeld and G. Kahl, J. Phys. Condens. Matter **9**, L89 (1997).

[20] I. M. Mryglod and V. V. Ignatyuk, J. Phys. Stud. (Ukraine) (to be published).

[21] A. B. Bhatia, D. E. Thornton, and N. H. March, Phys. Chem. Liq. **4**, 97 (1974).

[22] N. H. March and M. P. Tosi, *Atomic Dynamics in Liquids* (Macmillan Press, London, 1976).